

THE RADIO STRUCTURE OF HM SAGITTAE

SUN KWOK

Herzberg Institute of Astrophysics, Ottawa; and Department of Physics, University of Calgary, Calgary

R. C. BIGNELL

National Radio Astronomy Observatory,¹ Socorro, New Mexico

AND

C. R. PURTON

Dominion Radio Astrophysical Observatory, Penticton

Received 1983 May 23; accepted 1983 August 24

ABSTRACT

We report observations of the peculiar variable star HM Sge, made with the Very Large Array radio telescope. The nebula of HM Sge is spatially resolved, showing a diffuse halo surrounding a central shell about $0''.15$ in size. This nebular structure is explained by the interaction of stellar winds originating from the hot and cool components of the system. We suggest the visual brightening of HM Sge in 1975 was due to a decrease in circumstellar extinction and the subsequent ionization of the circumstellar nebula.

Subject headings: stars: circumstellar shells — stars: individual — stars: radio radiation

I. INTRODUCTION

HM Sagittae is one of the most remarkable variable stars in that it displays activity in every spectral band from X-rays to the radio wavelengths (for a summary of its properties, see Kwok 1982). Its sudden optical brightening in 1975 resembled the outburst of a classical nova, but unlike novae, it has remained (with minor variations) at maximum light ever since (Ciatti, Mammano, and Vittone 1979). The simultaneous presence of high-excitation emission lines (e.g., He II with IP = 54.4 eV, Ciatti, Mammano, and Vittone 1979) and photospheric absorption features (e.g., CO, H₂O, Puetter *et al.* 1978) characteristic of cool stars suggests a symbiotic system consisting of a hot star and a cool companion. The detection of strong infrared continuum emission and the $10\ \mu\text{m}$ silicate dust feature (Davidson, Humphreys, and Merrill 1978) implies that the cool component is a late M giant. Photometric monitoring of HM Sge (Slovak 1978; Taranova and Yudin 1980) shows variations with a period of ~ 1 yr, consistent with the M giant being a Mira variable.

Zanstra analysis of the emission lines suggests the hot component of HM Sge to have a temperature in excess of 5×10^4 K (Davidson, Humphreys, and Merrill 1978). Because of the high emission line to continuum intensity ratio, the stellar continuum is only marginally detectable (Feibelman 1982). In the visible region, a continuum can be detected (Davidson, Humphreys, and Merrill 1978) but this is probably due to recombination and free-free emission from the circumstellar nebula.

The fact that HM Sge is surrounded by an extensive circumstellar nebula is indicated by the detection of thermal radio emission (Kwok and Purton 1979, hereafter KP). Assuming the ionized gas is part of the M-giant wind that ejects the silicate dust, KP estimated a mass loss rate of

$2 \times 10^{-6} (V/35\ \text{km s}^{-1}) (D/1\ \text{kpc})^{3/2} M_{\odot}\ \text{yr}^{-1}$, where V and D are the wind velocity and the distance, respectively.

HM Sge represents an evolutionary system unique in many ways. The interrelationships between the hot component, the cool component, and the nebula are particularly intriguing. In this paper, we present high angular resolution radio observations of the nebula and suggest an evolutionary scenario to explain the present nebula structure.

II. OBSERVATIONS AND RESULTS

HM Sge was observed at the Very Large Array (VLA) of the National Radio Astronomy Observatory on 1982 February 16. The A configuration was used for maximum resolution. Measurements were made at all four standard VLA bands (20, 6, 2, and 1.3 cm). 1923+210 was observed every 15 minutes for calibration purposes. Absolute flux density calibration was obtained by observing 3C 286 at the beginning of the session. The total on-source integration time at each band is given in Table 1.

The source positions and angular sizes were determined by fitting elliptical Gaussian components to the calibrated visibility data. The results of these fittings with their corresponding $1\ \sigma$ formal errors are given in Table 1.

Figures 1a, 1b, and 1c show the visibility amplitudes as functions of projected baselines for 20, 6, and 2 cm, respectively. It is clear that HM Sge does not resemble a point source even at the longest wavelength of 20 cm (FWHP beamwidth = $1''.3$). Furthermore, fittings of elliptical Gaussian functions to the visibility data show that the angular size increases with increasing wavelength (Table 1). This suggests that the optically thick surface increases in size with wavelength, implying the existence of a density gradient in the circumstellar envelope.

The nonuniform density structure of the envelope can be tested by model fitting of the visibility data. We have calculated the theoretical visibility curves expected from a

¹ The National Radio Astronomy Observatory is operated by Associated Universities, Inc., under contract with the National Science Foundation.

TABLE 1
DERIVED POSITIONS, FLUX DENSITIES, AND ANGULAR SIZES OF HM SAGITTAE

WAVELENGTH (cm)	INTEGRATION TIME (minutes)	INTEGRATED FLUX DENSITY (mJy) ESTIMATED FROM			BEAM SIZE (")	MAJOR AXIS (")	MINOR AXIS (")	POSITION ANGLE (°)	$\alpha(1950)$	$\delta(1950)$
		Gaussian Fittings	Visibility Curve	Sum of CLEANed Components						
20	18	16.4 ± 0.6^a	19 ± 2	14 ± 1	1.3	0.88 ± 0.08	0.44 ± 0.14	62.1 ± 9.7	$19^h39^m41.519 \pm 0.002$	$16^\circ37'32''.91 \pm 0.02$
6	14	41.8 ± 0.3^a	45 ± 2	44 ± 1^b	0.4	0.40 ± 0.01	0.31 ± 0.01	50.1 ± 2.3	41.408 ± 0.001	33.04 ± 0.01
2	14	91 ± 3^a	130 ± 10	146 ± 3^b	0.13	0.22 ± 0.02	0.16 ± 0.03	177.9 ± 11.1	41.408 ± 0.001	33.01 ± 0.01
1.3	293	98 ± 4^a	150 ± 20	186 ± 10^b	0.07	0.36 ± 0.02	0.24 ± 0.01	89.6 ± 5.0	41.406 ± 0.001	33.02 ± 0.01

NOTE.—Observing date, 1982 February 16; A configuration of the VLA.

^a 1σ errors.

^b After self-calibration.

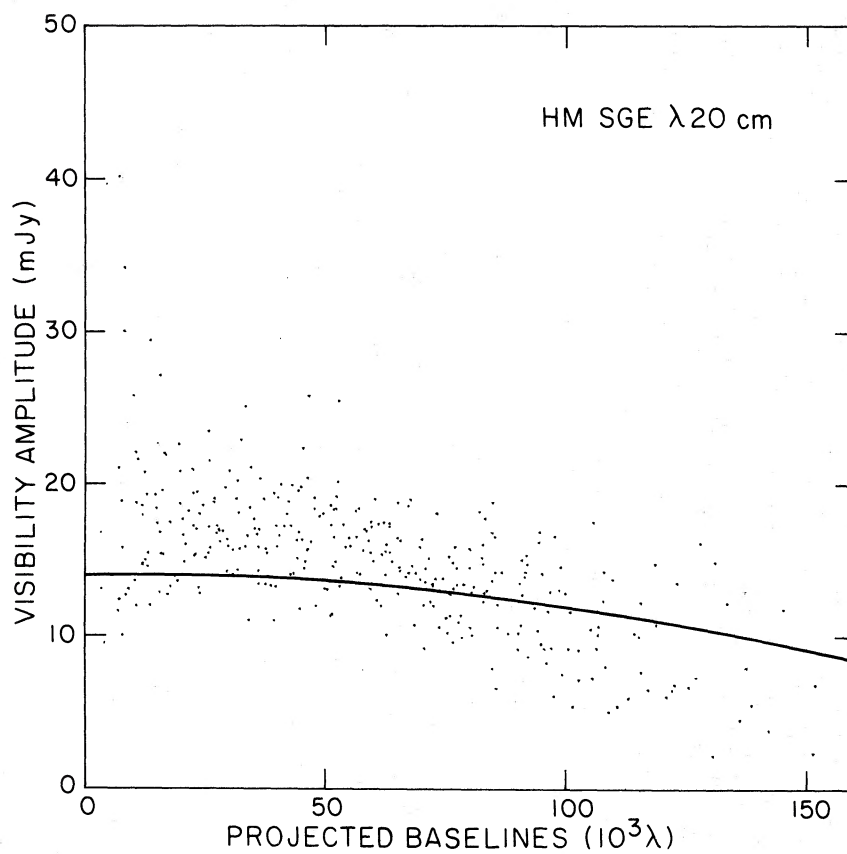


FIG. 1a

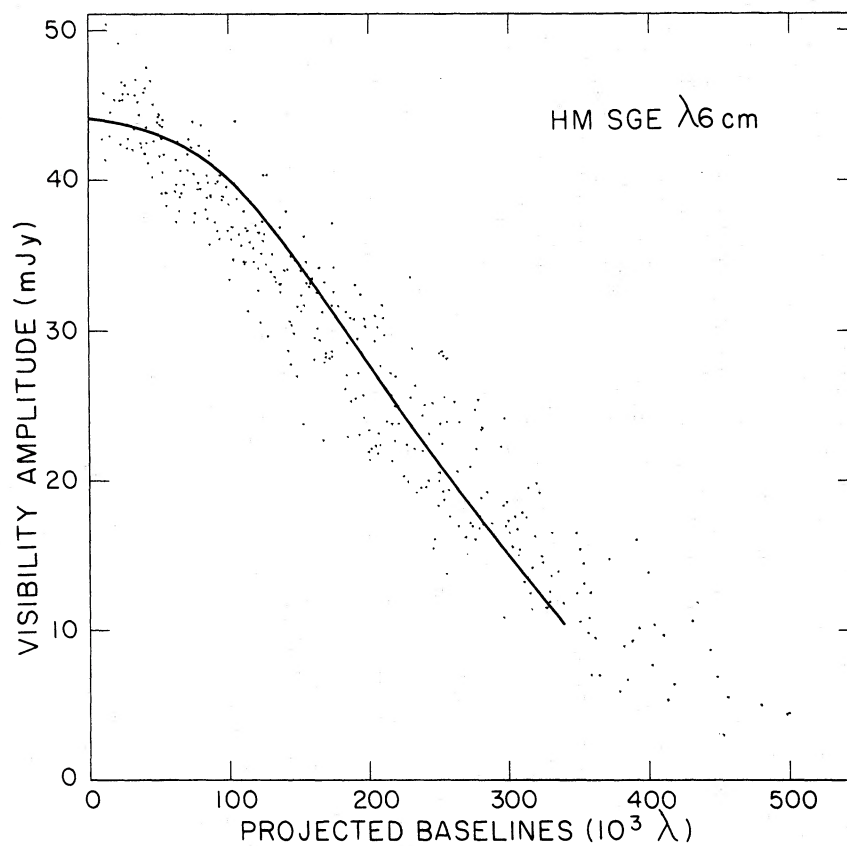


FIG. 1b

FIG. 1.—Visibility data of HM Sge at 20, 6, and 2 cm. The fringe amplitude is plotted against projected spacings within the array in units of wavelengths. Also plotted are the theoretical visibility curves for an ionized nebula of size 935 AU with an inverse-square-law density distribution ($n = 6 \times 10^{36} \text{ cm}^{-3} r^{-2}$).

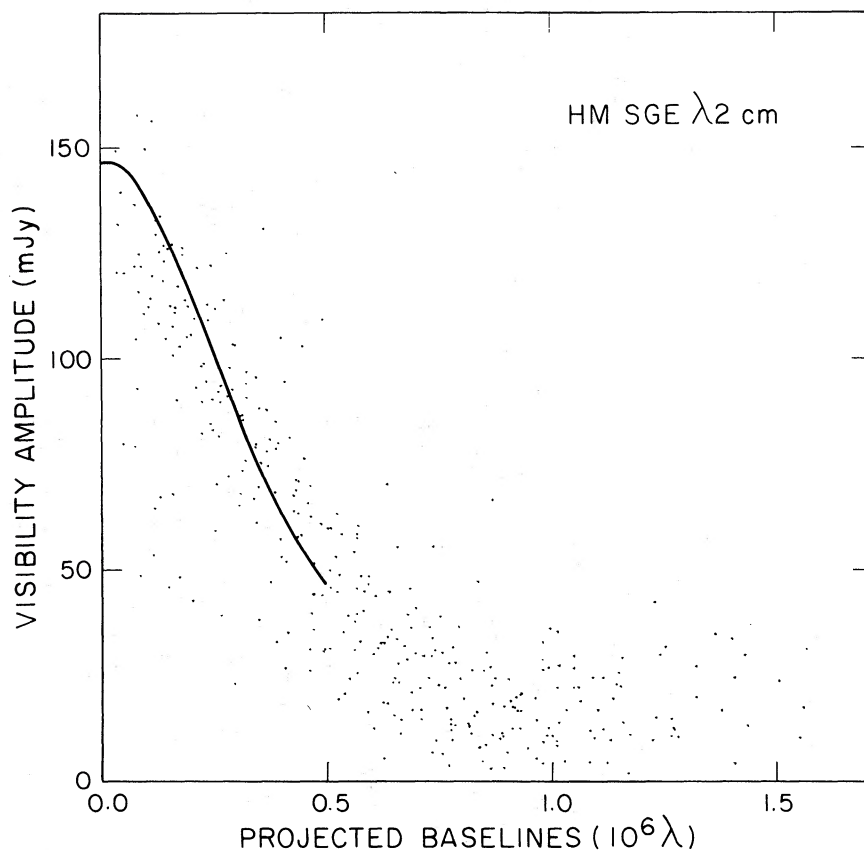


FIG. 1c

nebula of size R and a simple density law of the form $n = Ar^{-2}$. Results of these fits with parameters $R = 935$ AU and $A = 6 \times 10^{36} \text{ cm}^{-1}$ are plotted in Figures 1a, 1b, and 1c. These fits confirm the presence of a windlike density structure at least in the outer parts of the circumstellar envelope.

Because of the lower angular resolutions at 20 and 6 cm, there is no indication of source asymmetry in Figures 1a and 1b. However, the visibility curve at 1.3 cm shows clear deviations from circular symmetry. For this reason and the fact that the source is highly resolved we have omitted the visibility plot at 1.3 cm. The source structure can be better seen in the intensity map presented later in this section.

The visibility curve at 20 cm (Fig. 1a) shows large variations at short spacings ($< 5000\lambda$) which are significantly larger than the noise estimated from larger spacings. This is probably due to confusing effects from the nearby source OV +168, which is $\sim 17'$ away from HM Sge and is within the primary beam at 20 cm (FWHP beamwidth = $30'$). The confusion effect is minimized at larger spacings when OV +168 is spatially resolved.

The calibrated visibility data at each frequency band was also Fourier transformed into an intensity map which was then subjected to the CLEANing process (Clark 1980). We found that the dynamic range of the maps (particularly at 2 and 1.3 cm) can be significantly improved by the self-calibration procedure in which the CLEANed map is used as

a model to predict the phase observed by each antenna in each time interval (3 minutes in this case).

Figures 2a, 2b, and 2c show the intensity maps at 6, 2, and 1.3 cm, respectively. Figure 2c shows a double structure with two emission peaks separated by $0''.08$ along the NNW direction. This is consistent with the elongated structure seen in Figure 2b. The source is extended over $\sim 0''.5$ in the sky, but a steep brightness gradient around the central $0''.15$ of the source can be seen in Figure 2c. This suggests the existence of a high-density shell surrounded by a low-density halo.

The shell-halo structure is not obvious in Figures 2a and 2b probably because of the lower angular resolutions at 6 and 2 cm. It is also possible that the halo is optically thick in low frequencies and therefore obstructs the line of sight into the shell. However, low-brightness (~ 0.2 mJy per beam) emission can be seen over a $2''$ area in Figure 2a, suggesting that the halo may have a physical size over 10 times the size of the shell.

Because of the complicated source structure, reliable total flux densities cannot be determined by Gaussian fittings. This is true at high frequencies where the source is completely resolved and also true at low frequencies where the radial brightness distribution is probably non-Gaussian because of a density gradient in the halo. The formal fitting results presented in Table 1 must therefore be viewed with caution. An alternate method to obtain the total flux density is by

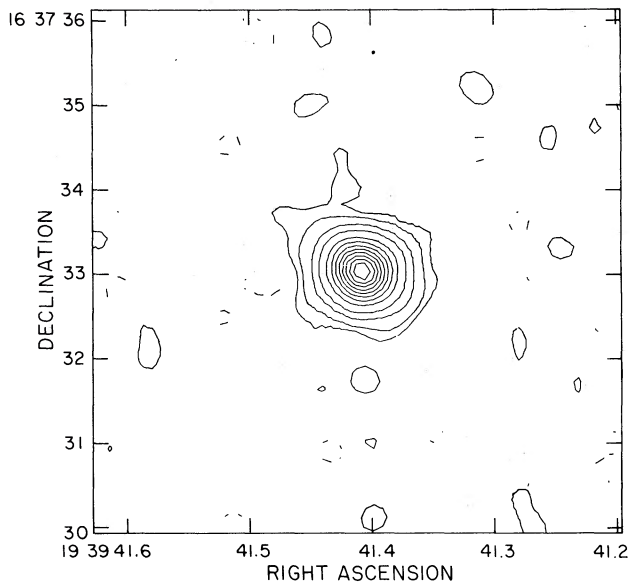


FIG. 2a

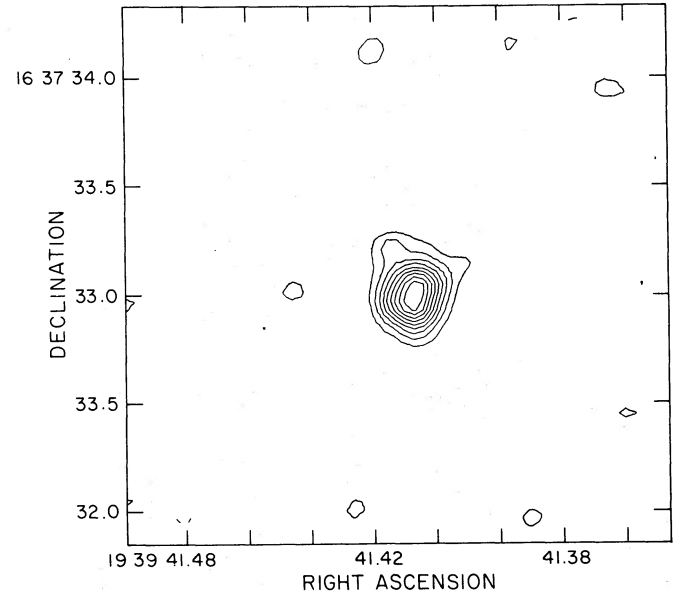


FIG. 2b

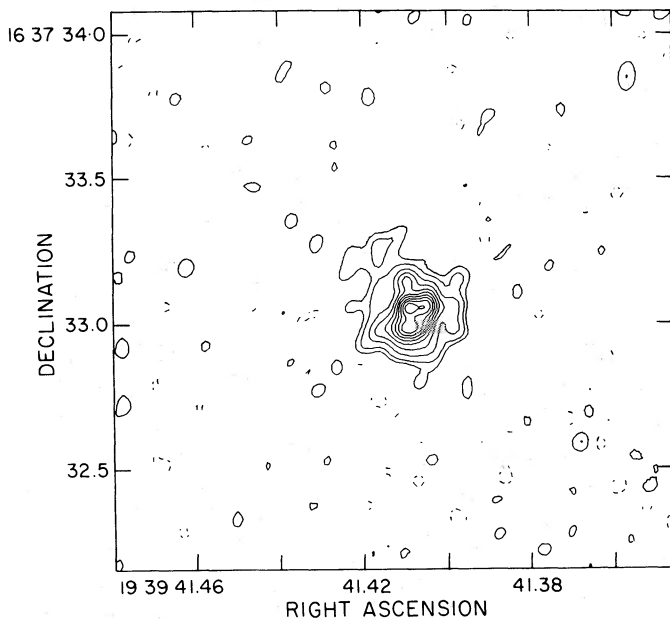


FIG. 2c

FIG. 2.—(a) Map of HM Sge at 6 cm after self-calibration. The map has been CLEANed to a level of 0.1 mJy per beam. Contours are at intervals of 10% of the peak value (peak flux = 23.4 mJy per beam) with additional contours at 1%, 2%, and 5% levels. The synthesized beam size is $0''.4$. (b) Map of HM Sge at 2 cm after self-calibration. The map has been CLEANed to a level of 0.1 mJy per beam. Contours are at 10% of the peak value (peak flux = 32.6 mJy per beam). Synthesized beam size is $0''.13$. (c) Map of HM Sge at 1.3 cm after self-calibration. The map has been CLEANed to a level of 0.5 mJy per beam. Contours are at 10% of the peak value (peak flux = 25.9 mJy per beam) with an additional contour at the 5% level. The synthesized beam size is $0''.07$.

summing all the components removed during the CLEANing process. Results obtained by this method (given in Table 1) are consistent with the zero-spacing visibility amplitudes inferred from the visibility curves (Fig. 1).

Figure 3 shows the spectrum of HM Sge in early 1982. The 2.8 cm measurement was made at the Algonquin Radio Observatory² on 1982 January 14. Also shown for comparison purposes are the spectra during 1977 and 1980 (Purton, Kwok, and Feldman 1983). A systematic brightening over this 5 year interval is evident.

Extrapolation of the ratio light curves of HM Sge suggests that the envelope will soon become optically thin as the result of expansion, and the radio emission will begin a phase of monotonic decline. Since the free-free opacity decreases with increasing frequency, this "turnover" will first become apparent at high frequencies. In fact, Figure 2c shows that the halo component was already optically thin at 1.3 cm in 1982. We can therefore generally predict that HM Sge will go through its maximum at centimeter wavelengths during 1983–1984.

III. DISCUSSIONS

What is the nature of HM Sge? The detection of molecular absorption bands and the observations of infrared variability suggest the cool components to be a Mira variable. This interpretation is also consistent with the presence of silicate dust (Davidson, Humphreys, and Merrill 1978), which is probably ejected from the M giant in the form of a stellar wind.

The hot (compact) component is not directly observable, and its properties can only be inferred indirectly. *IUE* observations (Feibelman 1982) have not been able to detect a definite stellar continuum, but the many emission lines (some with ionization potentials greater than 100 eV) indicate a stellar temperature of 10^5 K. The observed Wolf-Rayet

² The Algonquin Radio Observatory is operated by the National Research Council of Canada, Ottawa, as a national radio astronomy facility.

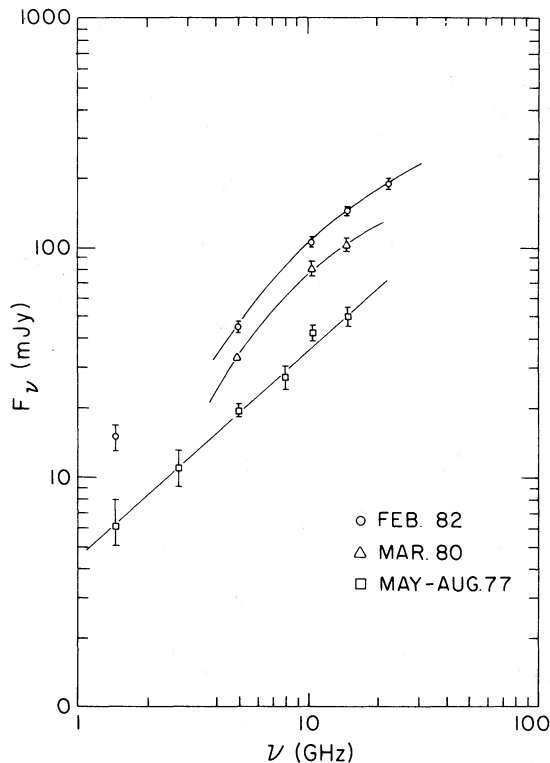


FIG. 3.—The radio spectra of HM Sge in 1977, 1980, and 1982. Eye-fitted lines are drawn through the data points of the same epoch to illustrate the radio brightening over the 5 year interval. The 1977 and 1980 points are taken from Purton, Kwok, and Feldman (1983).

features of velocities up to 2000 km s^{-1} (Wallerstein 1978; Belyakina, Gershberg, and Shakhovskaya 1978, 1979; Brown *et al.* 1978; Ciatti, Mammano, and Vittone 1978; Swings and Andrillat 1981) are best explained by a wind originating from the compact star. These properties suggest that the hot component is a hydrogen-shell-burning degenerate star similar to the central stars of planetary nebulae.

It is possible that the high-ionization lines result from dynamical heating by this wind but not by photoionization. If this is the case, then the Zanstra method of temperature determination is inappropriate, and the hot star may have a temperature much lower than 10^5 K .

Given the assumption that the HM Sge system consists of a cool Mira variable and a nuclear-burning carbon-oxygen white dwarf, we can then proceed to answer the following questions: (1) What is the cause of the visual brightening in 1975? (2) Can the nebular structure reported in the last section be produced by these stellar components?

a) The Visual Brightening

The total infrared flux from HM Sge is $\sim 9 \times 10^{-8} \text{ ergs cm}^{-2} \text{ s}^{-1}$ (cf. KP), which is significantly larger than the flux densities at all other wavelengths combined (see Fig. 4). This implies a total luminosity of $\sim 3 \times 10^3 (D/1 \text{ kpc})^2 L_{\odot}$. Since the lower luminosity limit for a 300 day Mira variable is $\sim 6 \times 10^3 L_{\odot}$ (Wood and Cahn 1977) and for a shell-burning white dwarf is $\sim 3 \times 10^3 L_{\odot}$ (core mass = $0.57 M_{\odot}$,

Paczynski 1971), the total luminosity of HM Sge must be $> 9 \times 10^3 L_{\odot}$. This translates to a minimum distance of 1.7 kpc. If one takes into account evolutionary considerations and argues that the degenerate component in a binary system must have a mass greater than the core mass of its companion, then the total luminosity would have to be $1.2 \times 10^4 L_{\odot}$ and the distance at least 2 kpc.

Let us adopt the above parameters and consider whether the visual brightening can be due to the onset of hydrogen shell burning on the white dwarf. A 300 day Mira variable should have a typical bolometric correction of ~ -4 , or $m_v \sim 11$ at $D = 2 \text{ kpc}$. Since the white dwarf is estimated to have an effective temperature as high as 10^5 K , its contribution to the visual brightness would be less than 10% of the cool component if they have the same intrinsic luminosities. Even if the temperature of the hot component is as low as $5 \times 10^4 \text{ K}$, its contribution is only a few tenths of a magnitude, and therefore it cannot be responsible for the 4 visual magnitudes increase in 1975. Furthermore, if the observed long-period IR variations (Taranova and Yudin 1980) are modulated by the pulsation of the Mira component, then the Mira variable must be the dominant source of heating of the dust and probably the major source of energy in the system.

Paczynski and Rudak (1980) suggest that the brightening of HM Sge is the result of a mild hydrogen shell flash, which could last for years for a low-mass star. In order to account for the brightening, a luminosity exceeding $2 \times 10^5 L_{\odot}$ is needed. Since most of the visible and ultraviolet fluxes of HM Sge are contributed by emission lines, it is clear that the continuum level of the hot star plays no part in the brightening process. The analogy to the outburst of a classical

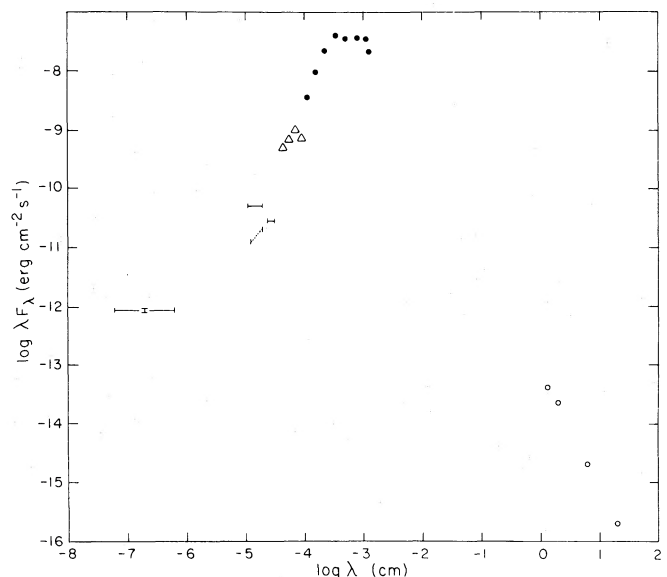


FIG. 4.—The energy distribution of HM Sge. The X-ray fluxes are taken from Allen (1981). The ultraviolet fluxes (at epoch 1981.2, for the SWP and LWR cameras of IUE) are taken from Feibelman (1982). The dotted line refers to the probable continuum level. The optical (Δ) and infrared (\bullet) fluxes are from Davidson, Humphreys, and Merrill (1978). The radio fluxes (\circ) are from this paper.

nova is therefore not appropriate because the nova maximum is almost totally due to continuum emission. In the case of HM Sge, the only function served by the hot component is as a source of ionizing photons, and a dramatic increase in luminosity is not necessary to explain the brightening.

An alternate explanation is offered by KP, who suggest that the brightening is due to the dissipation of the circumstellar dust and the subsequent ionization of the circumstellar gas envelope. Comparing the Mira m_v of 11 mag (for $D = 2$ kpc) with its pre-outburst visual magnitude of ~ 15 mag (Ciatti, Mammano, and Vittone 1977), one can conclude that a considerable amount of reddening must have been present before 1975. If we adopt the observed visual continuum ($m_v \sim 12$ mag; Davidson, Humphreys, and Merrill 1978) as an upper limit to the stellar continuum, then ≥ 1 mag of visual extinction should still be present after the outburst. This is consistent with the extinction derived from the Balmer lines ($A_v \sim 2-3$ mag in 1977, Davidson, Humphreys, and Merrill 1978; $A_v \sim 0.9-1.8$ mag in 1979, Blair *et al.* 1981; $A_v \sim 1.8 \pm 0.6$ mag in 1980, Thronson and Harvey 1981).³

We arrive at the following scenario for the visual brightening of HM Sge. Before 1975, the system consisted of a degenerate white dwarf and a Mira variable embedded in a dusty circumstellar envelope. Continued mass transfer through the Mira wind onto the white dwarf led to the ignition of hydrogen shell burning. A fast wind from the now luminous hot component began to sweep up the circumstellar gas and dust, greatly decreasing the envelope optical depth both in the visual and ultraviolet wavelengths. The observed $\frac{1}{2}$ yr brightening interval would then correspond to the time for the ionization front to propagate through the inner parts of the circumstellar envelope. Since the outer parts of the envelope can offer little resistance to the ionization front (cf. KP), the whole envelope is completely ionized by early 1976, creating a wealth of emission lines and a brighter visual magnitude.

b) The Nebular Structure

The shell-halo structure we find for HM Sge shows a resemblance to V1016 Cygni (Newell 1981). This is not surprising, since the two objects have similar histories of optical outbursts. The continuing radio brightening of HM Sge, however, suggests that the circumstellar nebula is optically thick at radio wavelengths and expanding. If one assumes the simplistic model of an expanding blackbody and compares the radio flux densities (S_ν) at two different epochs, the expansion velocity (V_s) can be estimated. For example, the 10.6 GHz flux densities of HM Sge are 41 ± 3 and 104 ± 4 mJy at 1977.49 and 1982.04, respectively. Assuming $T_e = 2 \times 10^4$ K (Blair *et al.* 1981), we have

$$\theta = \frac{\theta(1982) - \theta(1977)}{4.55 \text{ yr}} \\ \approx 0.024 \text{ arcsec yr}^{-1},$$

³ Thronson and Harvey (1981) derive a visual extinction of 12 ± 1 mag from the Brackett lines. Such a high value is probably due to the extrapolation from the infrared to the visual using an extinction curve inappropriate for the dust grains around HM Sge.

or

$$V_s = \frac{\theta D}{2} \approx 56 \left(\frac{D}{1 \text{ kpc}} \right) \text{ km s}^{-1},$$

where $\theta = (2c^2/\pi kT)^{1/2} S_\nu^{1/2} \nu^{-1}$ is the blackbody diameter at frequency ν . For $D \sim 2$ kpc, $V_s \sim 10^2$ km s⁻¹, which is generally consistent with line widths observed in HM Sge (Willson and Wallerstein 1981).

The above derived expansion velocity for HM Sge is much smaller than the expansion velocities of novae. This in part explains the long optically thick phase of ≥ 6 yr for HM Sge compared with those of novae, which typically last ~ 1 yr (Hjellming *et al.* 1979). While the radio light curves of novae can be understood as a simple wind process (Kwok 1983), the small expansion velocity of HM Sge demands an alternate explanation.

In the single-star model of KP, the optical, infrared, and radio properties of HM Sge are discussed in terms of an interacting stellar winds model. In particular, the radio emission is suggested to originate from the ionized red-giant circumstellar envelope, which is being swept up by a new wind from the exposed core of the red giant. While observational evidence now favors a binary-star model (Allen 1980), observations of the circumstellar nebula have confirmed the predictions of KP, which include the radio brightening and the shell-halo structure reported in this paper. This suggests that the interacting winds picture is still generally valid, but the origins of the stellar winds must be modified to fit in a binary system.

The silicate dust feature probably originates in the Mira component. If we identify the halo component in Figure 2c as the wind from the Mira variable, then the parameters we used in fitting the visibility curves of Figure 1 imply a mass loss rate of $10^{-5} (V/35 \text{ km s}^{-1}) M_\odot \text{ yr}^{-1}$. This value is comparable to the mass loss rates commonly observed in Mira variables. Recent ultraviolet observations have also found high-velocity winds ($v \sim 2000$ km s⁻¹) from central stars of planetary nebulae (Heap 1982). Since the hot component is a shell-burning white dwarf similar to central stars of planetary nebulae, the emergence of a stellar wind after the commencement of nuclear burning is therefore not unreasonable. The mass loss rate required ($\sim 5 \times 10^{-7} M_\odot \text{ yr}^{-1}$) is indeed similar to values observed in central stars of planetary nebulae.

Figure 5 shows a schematic diagram of the interacting winds model. The separation of the two stars ($< 10^{14}$ cm) is greatly exaggerated in relation to the size of the red-giant envelope ($\sim 5 \times 10^{16}$ cm). The dense shell formed at the interface of the two winds is similar to planetary nebula shells, except it receives its energy and mass separately from the two stars. Although we expect a certain degree of asymmetry in the shell during the early stages of its formation (as indicated in Fig. 5), this asymmetry should disappear as the shell expands because of the small separation between the two stars compared with the size of the circumstellar envelope. The asymmetry that we observe in Figure 2c can be due either to this effect or to an anisotropic density distribution in the red-giant envelope due to rotation (Calvet and Peimbert 1983). Orbital motion of the binary system may also introduce complications to the two-dimensional diagram shown in Figure 5.

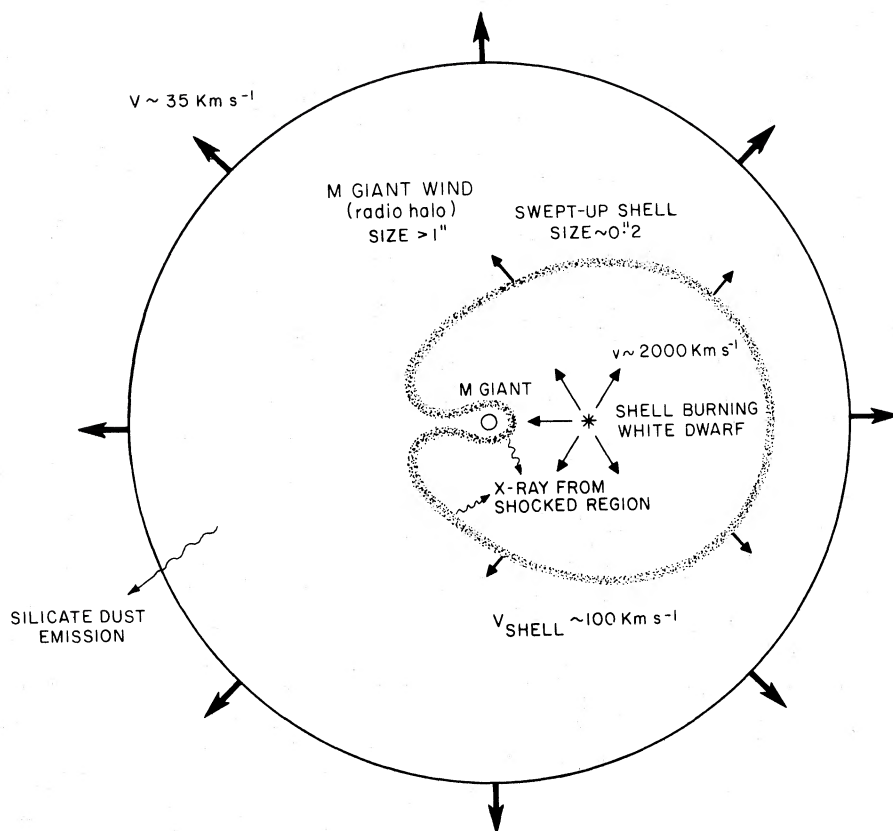


FIG. 5.—A schematic diagram (not to scale) showing the interacting stellar winds model of HM Sge

c) Evolutionary Considerations

The unusual spectral characteristics and the unique radio brightening of HM Sge can be attributed to the fact that the cool component is a star in the very late stages of evolution. Rather than being a main-sequence dwarf as in classical novae, the cool component is bolometrically bright and has a strong wind of its own. The combination of these two characteristics leads to an optical history which is significantly different from that of ordinary novae and an extremely slow spectral evolution in the radio wavelength.

The fact that one component of HM Sge is a carbon-oxygen white dwarf suggests that the original separation must be very wide—enabling the more massive component (the primary) to evolve independently and develop a C-O core. The evolution of the secondary to a Mira variable can also be the result of independent evolution, which implies that it has a main-sequence mass comparable (but smaller) to its companion. It is possible that the secondary benefited from mass transfer while the primary was a red giant, and the evolution of the secondary to the present Mira phase was hastened as a result. The importance of this mass transfer cannot be assessed accurately for it is equally probable that most of the hydrogen envelope of the primary was lost to the interstellar medium via a stellar wind during the asymptotic giant branch and the planetary nebula phases. It is therefore possible that HM Sge represents an evolutionary process more extreme than the case C binary evolution

considered by Paczyński (1980), and this interacting binary system of two very evolved stars may provide an interesting laboratory for the study of stellar evolution.

IV. CONCLUSIONS

High angular resolution VLA observations of HM Sge have revealed a shell-halo structure in its circumstellar nebula. The halo component can be identified with a stellar wind from the M-giant component, which is in the process of being swept up by a new fast wind initiated after the onset of nuclear burning on the white dwarf component in 1975. The observed dense shell of size $\sim 0''.15$ is probably the result of the interaction of the two winds.

The overall energy distribution of HM Sge from X-ray to the radio shows that most of the energy is emitted in the infrared. Since the infrared emission seems to be modulated by the pulsations of the Mira variable, it is likely that the Mira variable is the brighter of the two components in the system. This suggests that the visual brightening of HM Sge in 1975 is due to the ionization of the circumstellar envelope rather than to a dramatic increase in the continuum level of the hot component.

HM Sge is expected to achieve its radio maximum in 1983–1984, and we plan to continue to monitor the evolution of its radio spectrum.

We would like to thank Ms. Peggy Perley, who skillfully calibrated most of the data presented here. S. K. also wishes to thank Dr. Philipp Kronberg for use of the VLA data

reduction facility at the University of Toronto, and Dr. L. A. Willson for helpful discussions.

REFERENCES

- Allen, D. A. 1980, *M.N.R.A.S.*, **192**, 521.
 ———. 1981, *M.N.R.A.S.*, **197**, 739.
 Belyakina, T. S., Gershberg, R. E., and Shakhovskaya, N. I. 1978, *Soviet Astr.—AJ Letters*, **4(5)**, 219.
 ———. 1979, *Soviet Astr.—AJ Letters*, **5(6)**, 349.
 Blair, W. P., Stencel, R. E., Shaviv, G., and Feibelman, W. A. 1981, *Astr. Ap.*, **99**, 73.
 Brown, L. W., Feibelman, W. A., Hobbs, R. W., and McCracken, C. W. 1978, *Ap. Letters*, **19**, 75.
 Calvet, N., and Peimbert, M. 1983, *Rev. Mexicana Astr. Ap.*, Vol. 5, No. 4, p. 319.
 Ciatti, F., Mammano, A., and Vittone, A. 1977, *Astr. Ap.*, **61**, 459.
 ———. 1978, *Astr. Ap.*, **68**, 751.
 ———. 1979, *Astr. Ap.*, **79**, 247.
 Clark, B. G. 1980, *Astr. Ap.*, **89**, 377.
 Davidson, K., Humphreys, R. M., and Merrill, K. M. 1978, *Ap. J.*, **220**, 239.
 Feibelman, W. A. 1982, *Ap. J.*, **258**, 548.
 Heap, S. R. 1982, in *IAU Symposium 99, Wolf-Rayet Stars: Observations, Physics and Evolution*, ed. C. W. H. de Loore and A. J. Willis (Dordrecht: Reidel), p. 423.
 Hjellming, R. M., Wade, C. M., Vandenberg, N. R., and Newell, R. T. 1979, *A.J.*, **84**, 1619.
 Kwok, S. 1982, in *IAU Colloquium 70, The Nature of Symbiotic Stars*, ed. M. Friedjung and R. Viotti (Dordrecht: Reidel), p. 209.
 ———. 1983, *M.N.R.A.S.*, **202**, 1149.
 Kwok, S., and Purton, C. R. 1979, *Ap. J.*, **229**, 187 (KP).
 Newell, R. T. 1981, Ph.D. thesis, New Mexico Institute of Mining and Technology.
 Paczyński, B. 1971, *Acta Astr.*, **21**, 417.
 ———. 1980, *Highlights of Astronomy*, **5**, 27.
 Paczyński, B., and Rudak, B. 1980, *Astr. Ap.*, **82**, 349.
 Puetter, R. C., Russell, R. W., Soifer, B. T., and Willner, S. P. 1978, *Ap. J. (Letters)*, **223**, L93.
 Purton, C. R., Kwok, S., and Feldman, P. A. 1983, *A.J.*, **88(12)**, 1925.
 Slovak, M. H. 1978, *Astr. Ap.*, **70**, L75.
 Swings, J. P., and Andrillat, Y. 1981, *Astr. Ap.*, **103**, L3.
 Taranova, O. G., and Yudin, B. F. 1980, *Soviet Astr.—AJ Letters*, **6(4)**, 273.
 Thronson, H., and Harvey, P. M. 1981, *Ap. J.*, **248**, 584.
 Wallerstein, G. 1978, *Pub. A.S.P.*, **90**, 36.
 Willson, L. A., and Wallerstein, G. 1981, paper presented at the North American Workshop on Symbiotic Stars, Boulder, Colorado.
 Wood, P. R., and Cahn, J. H. 1977, *Ap. J.*, **211**, 499.

R. C. BIGNELL: National Radio Astronomy Observatory, P.O. Box 0, Socorro, NM 87801

S. KWOK: Department of Physics, The University of Calgary, Calgary, Alta. T2N 1N4, Canada

C. R. PURTON: Dominion Radio Astrophysical Observatory, P.O. Box 248, Penticton, B. C. V6A 2K4, Canada